

# ZNO-CARBON COMPOSITES AND IMPRINTED CARBON MATERIALS VIA PYROLYSIS OF $\text{ZnCl}_2$ -CATALYZED FURFURYL ALCOHOL POLYMERS

*Federico Cesano, Domenica Scarano, Serena Bertarione, Alessandro Damin, Francesca Bonino, Silvia Bordiga, and Adriano Zecchina,*

*Dept. of Inorganic, Physical and Materials Chemistry, NIS (Nanostructured Interfaces and Surfaces) Centre of Excellence, University of Torino, Via P. Giuria 7, Torino, Italy, I-10125*

## Abstract

The sequential synthesis of C/ZnO composites and imprinted porous-C materials, from mixtures of  $\text{ZnCl}_2$  and furfuryl alcohol (FA) precursors, is reported. Acting as a Lewis acid catalyst,  $\text{ZnCl}_2$  promotes the polymerization of FA at 60-70°C. Upon temperature increasing (100-600°C,  $\text{N}_2+\text{O}_2$  ppm) FA polymers pyrolyze, but Zn (II) species remain in the matrix. As a result, the material obtained at 600 °C becomes fully covered by an uniform film of ZnO microcrystals that are implanted on the carbonaceous matrix. The surface of the underlying C-support is characterized by the presence of holes, whose size and shape are related to those of ZnO microcrystals. Further heating treatments at higher temperature (600-800°C,  $\text{N}_2+\text{O}_2$  ppm), lead to an imprinted C-material, where ZnO phase disappeared after reacting with the C-phase. The materials, obtained by pyrolysis process, have been investigated by TPD, FTIR, SEM, AFM, XRD and Raman. The effect of  $\text{ZnCl}_2$  concentration on the process of ZnO and C-phase formation, has been studied in detail.

## Introduction

Porous carbons are usually prepared by pyrolysis of polymers. Polyacrylonitrile (PAN), phenolic resin, polyimides, poly(p-phenylene vinylene), polyvinyl acetate and polyfurfuryl alcohol (PFA) are some of the most commonly used precursors [Pierson, 1993]. Among them, PFA (obtained by acid catalyzed polymerization of the monomer) provides a relatively high carbon yield (50-55%) [Pierson, 1993] and gives rise to amorphous carbons that are characterized by the presence of defects along the graphene sheets, such as pentagons, heptagons, vacancies, impurities and other non-hexagonal rings [Petkov, DiFrancesco, 1999, Strano, Zydney, 2002, Zarbin, Bertholdo, 2002]. The amorphous carbons retain their structures up to very high treatment temperatures (2500-3000°C) before to be converted into graphitic structures.

The polymerization of furfuryl alcohol (FA) is acid-catalyzed. Catalytic systems commonly reported in literature are:

- (i) mineral ( $\text{H}_2\text{SO}_4$ , etc.) and organic (p-toluenesulphonic, etc)acids [Pierson, 1993, Principe, 1999, Vergunst, 2002],
- (ii) acid zeolites (HY, HZSM-5) [Rodriguez-Mirasol, 1998, Stiel, 1999]
- (iii) Lewis acids ( $\text{SnCl}_4$ ,  $\text{TiCl}_4$ ) [Gonzalez, 2002].

In this work, we have investigated the catalytic effect of a Lewis acid ( $\text{ZnCl}_2$ ) on the polymerization of FA and the fate of the catalysts dispersed in the polymeric matrix upon thermal treatments in the 70-800 °C interval under  $\text{N}_2$  ( $\text{O}_2$  ppm) atmosphere treatment.

## Methods

PFA resins have been obtained by dissolving 5% w/w of  $\text{ZnCl}_2$  in liquid FA at room temperature. By stirring the mixture under mild conditions (80°C) a rapid polymerization of FA with subsequent formation of a brown, highly viscous, phase of PFA is observed. During this stage,  $\text{ZnCl}_2$  (or its hydrolysis products) remains dispersed into the polymeric matrix. Pyrolysis treatment have been performed under 100 ml/min  $\text{N}_2 + \text{O}_2$  ppm gas flow at 200°C, 400°C, 600°C and 800°C.

Samples, coming from the different temperature treatments, have been characterized by means of: FTIR spectroscopy (Perkin-Elmer Spectrum Spotlight 300 FTIR microscope), SEM microscopy (Leica Cambridge Stereoscan 420), AFM microscopy (Park Scientific Instrument Auto Probe LS), Raman spectroscopy (*Renishaw in Via Raman Microscope spectrometer* emitting at 514), XRD analysis (Philips PW3020 diffractometer,  $\text{Cu K}_\alpha$  radiation in a standard Bragg-Brentano geometry). TPD analysis (Hyden Catlab) have been performed on PFA obtained after polymerization upon thermal treatment at 70°C.

## Results and discussion

In the last decades many efforts have been devoted to understand the acid-catalyzed polymerization of furfuryl alcohol. It is known that the general mechanisms of the polymerization can be summarized as follows:

- i) reaction occurring between  $-\text{CH}_2\text{OH}$  groups and C-H of two adjacent FA molecules to form  $\text{CH}_2$ -linked furan rings (oligomerization) [Dunlop and Peters, 1953];
- ii) reaction occurring between  $-\text{CH}_2\text{OH}$  groups of two adjacent FA molecules to form  $\text{H}_2\text{C-O-CH}_2$ -linked furan rings (condensation) [Dunlop and Peters, 1953];
- iii) formation of conjugated chain species via-carbocation rearrangement of double bonds [Bertarione, 2007] (data not shown for sake of brevity), responsible for the polymer intense colouring [Choura, 1996].

We do not speculate anymore on the polymerization of FA, which is a complex process and cannot be limited only to a linear polymerization phenomenon occurring at 2,5-ring position. According to a such strict definition, many products could not be properly defined as PFA resins, because they could form other products, coming from side reactions simultaneously occurring with PFA formation.

The resulting viscous and coloured material contains not only randomly type i) and ii) chain sequences, whose double bonds can be redistributed to form conjugated species, but also chain sequences coming from furan ring opening [Conley and Metil, 1963] if treated at relatively high temperatures.

When the so-obtained resin is thermal treated by gradual temperature increasing (RT-800°C) under a flow of inert gas, the material becomes rigid and more dark coloured. Upon the pyrolysis process, volatile species are released. In Fig. 1 the TPD analysis is shown. In this figure two distinct regions are shown, where volatile species are released. In the first one (RT-250°C), water goes out from the polymer, which is still resinificating. At higher temperature (300-600°C), besides water other volatile species, are detected ( $\text{CO}$ ,  $\text{CO}_2$ ,  $\text{CH}_4$ , other hydrocarbons). After gas evolution upon pyrolysis, the formation of an amorphous carbon, is commonly accepted in literature [Foley, 1995, Pierson, 1993].

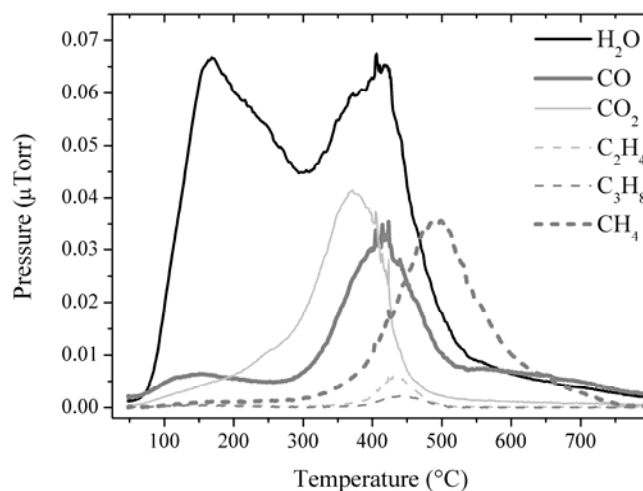


**Figure 1.** TPD analysis of PFA/Zn (II) composite, obtained from FA+  $\text{ZnCl}_2$  5% w/w, under He gas flow in the RT-800°C temperature range.

A further support to of the carbon formation, comes from IR investigation of materials obtained at different stages of pyrolysis (70°C, 200 °C, 400 °C, 600 °C and 800°C) under  $\text{N}_2$  ( $\text{O}_2$  ppm) atmosphere, as shown in Fig. 2. In this figure, the progressive evolution of IR bands is reported. In particular, IR spectrum of sample polymerized at 70°C (curve b) is compared to that of liquid FA at RT (curve a). More in detail:

- i) the broad absorption at  $3402\text{ cm}^{-1}$  is related to the stretching mode of the  $-\text{OH}$  ending groups of the PFA polymer chains, even if adsorbed water can contribute to the total intensity. This band is weaker than that of pure FA, which has one  $-\text{OH}$  group every furan ring [Choura, 1996],
- ii) the bands at  $2923$  and  $1422\text{ cm}^{-1}$ , assigned to  $-\text{CH}$  stretching and  $-\text{CH}$  scissoring vibrational modes of aliphatic  $-\text{CH}_2$  groups, are present in both cases,
- iii) the bands at  $1020$ ,  $1149$  and  $3125\text{ cm}^{-1}$ , assigned to C-O-C and C-H aromatic stretching modes, are the typical fingerprint of the furan ring present in FA and PFA,
- iv) peaks at  $793\text{ cm}^{-1}$ , related to 2,5-disubstituted furan rings [Choura, 1996], not found in IR spectrum of FA, is confirming the occurrence of the oligomerization process, whereas 2-monosubstituted furan heterocycles are present as well (band at  $735\text{ cm}^{-1}$ ) [Choura, 1996],
- v) the broad band appearing at  $1715\text{ cm}^{-1}$  in the IR spectrum of PFA, which has been assigned to C=O band, suggests a the occurrence of some ring-opening probably induced by the acidic medium [Choura, 1996], whose product has been ascribed to a polymer sequence containing the ester of levulinic acid [Sugama, 1985].

As far as the Zn species are concerned during the polymerization, their fate seems to be correlated with carboxylate anions species ( $\text{COO}^-$ ), whose typical bands are at  $1560\text{ cm}^{-1}$  and at  $1420\text{ cm}^{-1}$ . The formed product of polymerization is well compatible with Zn-FA chelate compounds. [Sugama, 1985].

Sample treated at  $200^\circ\text{C}$  (curve c) shows a weaker IR spectrum. By considering the fingerprint modes previously assigned to PFA, the band at  $\sim 790\text{ cm}^{-1}$  becomes stronger and broader, hence we speculate that polymerization is going on with the 2,5-disubstitution of furan rings. It is worthy noticing that  $\text{C}=\text{O}$  stretching frequency of the polymer ( $1710\text{ cm}^{-1}$ ) decreases upon hydrogen bond formation through the carbonyl oxygen [Sugama, 1985] and that  $-\text{CH}_2$  and  $-\text{CH}$  bonds of the ring disappear at increasing temperature of treatment, in accordance with literature data [Wang, 1998].

IR spectrum of sample treated at  $400^\circ\text{C}$  (curve d) exhibits different features. Besides  $-\text{OH}$  and aliphatic  $-\text{CH}_2$  vibrational modes ( $3515$ ,  $2921$  and  $1433\text{ cm}^{-1}$ , respectively), three broad bands appear with maxima at  $1706$ ,  $1603$ , and  $1220\text{ cm}^{-1}$ , respectively. The evolution of IR bands in the  $1700\text{--}1500\text{ cm}^{-1}$  range is typical of  $\text{C}=\text{C}$  stretching modes of neutral and charged conjugated species of variable length. It is worthy noticing that the bands at  $1020$ ,  $1149$  and  $3125\text{ cm}^{-1}$ , previously assigned to furan ring fingerprints, have disappeared. This means that at this temperature, even if FA fragments are still present, polymer chains coming from the furan ring opening, are formed and can rearrange to form aromatic C-C ring sequences.

IR spectrum of the sample treated at  $600^\circ\text{C}$  (curve e) shows an apparent oversimplification. As the  $-\text{OH}$  and aliphatic  $-\text{CH}_2$  vibrational modes fully disappear, two new and very broad bands, at  $1598$  and  $1250\text{ cm}^{-1}$ , are emerging. The first band is located very close to the  $E_{1u}$  band of graphite ( $1588\text{ cm}^{-1}$ ) and it might have been covered by the long tail between  $1750\text{--}1500\text{ cm}^{-1}$  interval [Wang, 1998]. The second very broad band ( $1250\text{ cm}^{-1}$ ) is attributed to the CH in-plane deformation along C-aromatic domains [Wang, 1998]. This fact can be debated considering that the advancing pyrolysis can open polymer crosslinking, whose terminations form C-aromatic domains as soon as volatile species, containing heteroatoms ( $\text{CO}$ ,  $\text{CO}_2$ ) and small fragments ( $\text{CH}_4$ , hydrocarbons, *vide supra*), are released.

IR spectrum of samples treated at  $800^\circ\text{C}$  (curve f) is very weak and no information about the carbonization process can be argued.

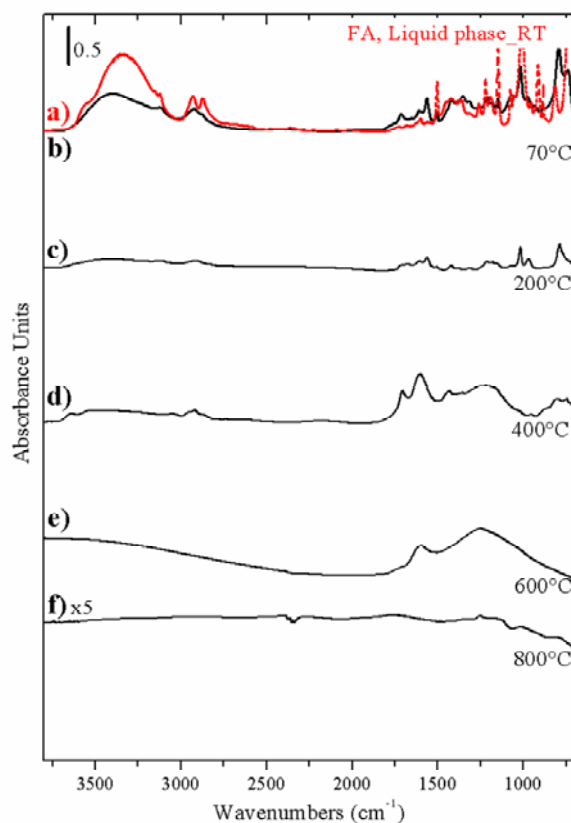


**Figure 2.** IR spectra of liquid FA (curve a), of sample polymerized at  $70^\circ\text{C}$  (curve b), and of samples treated under  $\text{N}_2$  ( $\text{O}_2$  ppm) atmosphere  $200^\circ\text{C}$  (curve c),  $400^\circ\text{C}$  (curve d),  $600^\circ\text{C}$  (curve e) and at  $800^\circ\text{C}$  (curve f), respectively.

Samples treated at  $600^\circ\text{C}$  and  $800^\circ\text{C}$  for 5h under  $\text{N}_2$  ( $\text{O}_2$  ppm) have been characterized by means of SEM, AFM, Raman and XRD analyses. SEM image of sample treated at  $600^\circ\text{C}$  is shown in Figure 3a. In this figure, a compact and homogeneous

layer of randomly oriented ZnO microcrystals lying on the carbon matrix is shown, whose terminations are imaged by AFM (Inset of Figure 3a). From this figure, regular extended prismatic and hexagonal faces are illustrated. The fact that crystals are formed by ZnO is confirmed from Raman and XRD analyses. In Figure 3b, Raman spectrum is reported. Besides the G ( $1580\text{ cm}^{-1}$ ) and D ( $1350\text{ cm}^{-1}$ ) bands, typical of an amorphous carbon with turbostratic structure [Robertson, 2002], also additional modes in the  $600\text{--}300\text{ cm}^{-1}$  range are observed. The broad and weak features in the  $600\text{--}500\text{ cm}^{-1}$  range can be assigned to E1 (LO) and A1 (LO) longitudinal phonon optical modes of ZnO, while the sharp peak at  $436\text{ cm}^{-1}$  is related to the first order frequency of E2 mode [Calleja and Cardona, 1977]. Further support to the formation of a C/ZnO composite comes from XRD analysis. The XRD pattern of the sample obtained at  $600^\circ\text{C}$  reveals two broad diffraction peaks (maxima at  $2\theta = 24.5^\circ$  and  $43.3^\circ$ ) and five narrower peaks (at  $2\theta = 31.7^\circ$ ,  $34.4^\circ$ ,  $36.2^\circ$ ,  $47.5^\circ$  and  $56.5^\circ$ ). The two broad peaks are assigned to the (002) and (100) diffraction planes of a turbostratic carbon phase [Johnson and Tison, 1969]. The narrow peaks are ascribed to the (100), (002), (101), (102) and (110) diffraction planes of wurzite ZnO phase. From the peak broadening and by using Sherrer's equation [Birks, 1946], the size of scattering coherent domains along the c-axis of the C-phase and along the (101) direction of the ZnO phase, have been found to be  $L_c = 1.6\text{ nm}$  and  $\approx 130\text{ nm}$ , respectively.

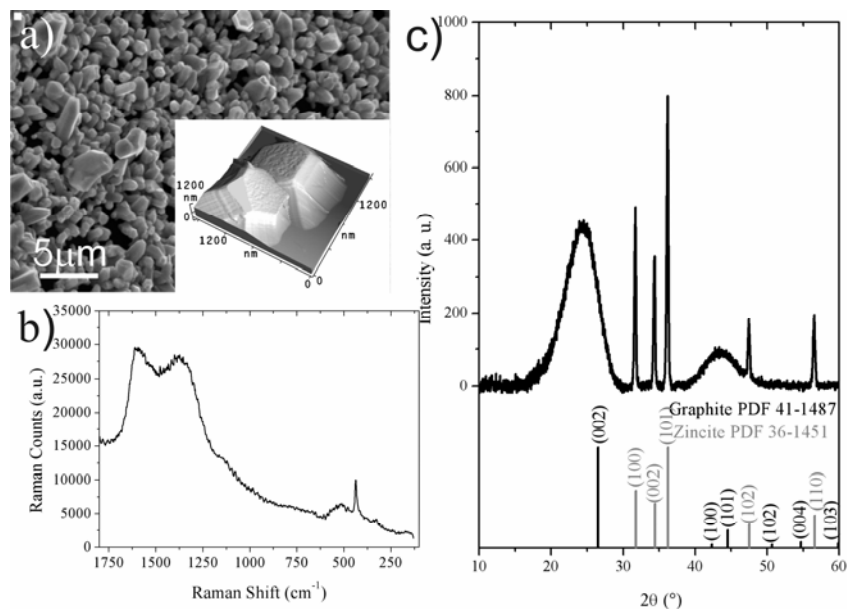


**Figure 3.** a) SEM/AFM, b) Raman and c) XRD analyses of sample obtained after thermal treatment at  $600^\circ\text{C}$  under  $\text{N}_2$  ( $\text{O}_2$  ppm) atmosphere.

SEM image of the sample treated at  $800^\circ\text{C}$  is shown in Fig. 4a. In this picture, the carbon phase surface clearly shows the presence of holes (inset in the upper part), whose topography is imaged by AFM (inset in the lower part). More insights on the occurring of the carbon phase come from Raman and XRD analyses. In Fig. 4b, Raman spectrum exhibits two broad bands at  $1580\text{ cm}^{-1}$  and  $1350\text{ cm}^{-1}$ , previously ascribed to G and D carbon bands of a non graphitizing carbon (turbostratic), formed under the adopted temperature of treatment [Robertson, 2002, Zerbi, 2006]. The XRD pattern of the sample obtained at  $800^\circ\text{C}$  reveals the two broad diffraction peaks (maxima at  $2\theta = 23.9^\circ$  and  $43.6^\circ$ ) related to (002) and (101) diffraction planes of the carbon phase. Note that the full width at half maximum (FWHM) of XRD diffraction bands remains very similar to those of C-phase of C/ZnO composite. This fact can be accounted for the structural order of such C-materials that becomes graphitic only at very high temperature ( $2500\text{--}3000^\circ\text{C}$ ) [Pierson, 1993].

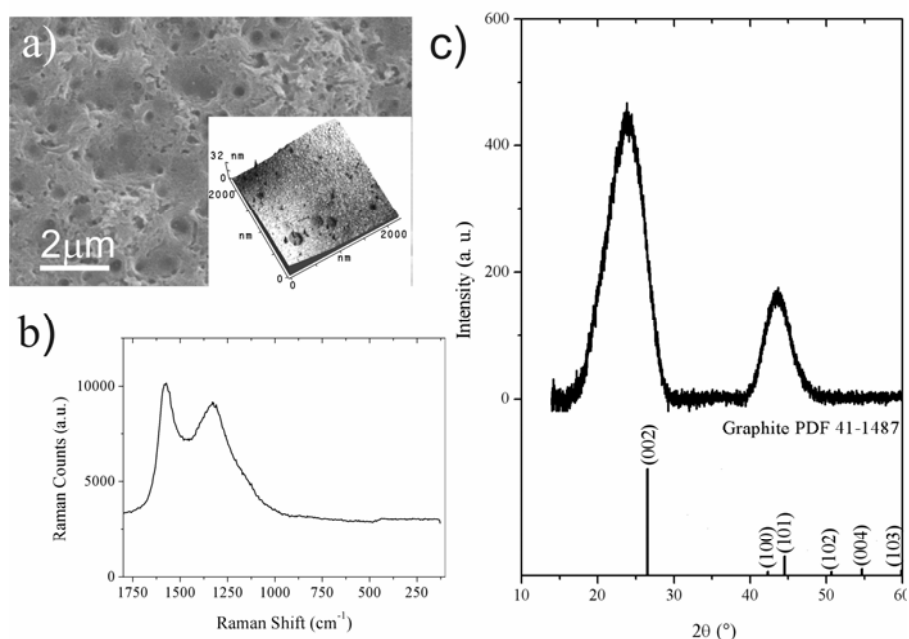
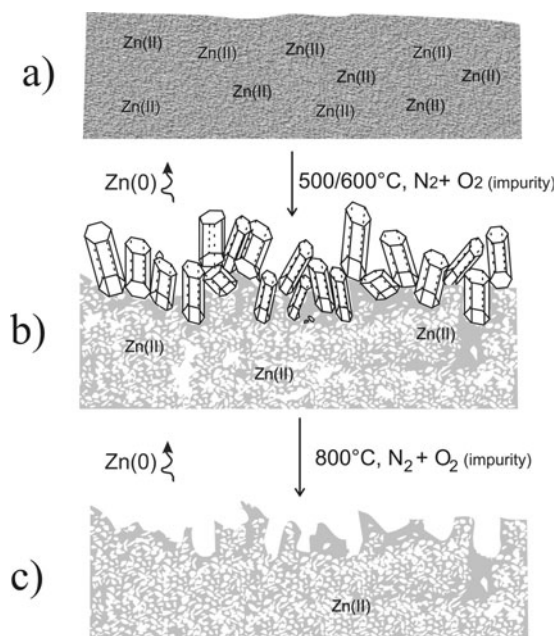


**Figure 4.** a) SEM/AFM, b) Raman and c) XRD analyses of sample obtained after thermal treatment at 800°C under N<sub>2</sub> (O<sub>2</sub> ppm) atmosphere.

An explanation of the process, can be proposed in Scheme 1. Zn(II)/PFA composite is plausibly the main product of polymerization a), which pyrolyzes upon increasing thermal treatment to form an amorphous carbon covered by a homogeneous film of ZnO microcrystals at 600°C implanted in the carbon phase b). The development of the ZnO phase can be ascribed to the presence of vapours of metal Zn (at  $T \geq \approx 500^\circ\text{C}$ ) coming from the bulk material, where reduction processes take place (carbon phase is forming). As soon as metal Zn meets the external flow, which contains O<sub>2</sub> as impurity, is immediately oxidized to ZnO. When the temperature is higher enough, ZnO phase can be reduced again to Zn (0), which goes out from the surface leaving a holed C-surface c), which remembers the presence of the ZnO crystals before formed. We do not exclude that the size of the holes is also partially determined by the consumption of the carbon in direct contact with the ZnO particles.

Further support to the effects of the ZnCl<sub>2</sub> on the morphology and on the porosity have been reported [Cesano, 2007], but here not shown for sake of brevity.



**Scheme 1.** Schematic representation of main products obtained from the process of FA polymerization ZnCl<sub>2</sub> acid-catalyzed and then pyrolysis : PFA/Zn(II) composite a), C/ZnO composite (500°C) b), C-porous material, with imprinted surface c).

## Conclusions

The process of polymerization and carbonization of a ZnCl<sub>2</sub>/FA mixture has been studied in detail by means of several techniques (IR, TPD, SEM, AFM, Raman and XRD). The preparation of microporous carbons is obtained through several stages, leading to the initial formation of PFA/Zn(II) composite (through the action of the Zn<sup>2+</sup> Lewis acid catalyst), carbon/ZnO composite and then to a pure porous carbon phase. For T < 400-500°C, Zn(II) remains dispersed in the carbonaceous matrix. For T ≅ 500°C or more, metal Zn is formed and migrates at the surface of the carbon as vapour, where by contacting the O<sub>2</sub> impurities, film is formed which is characterized by ZnO microcrystals implanted in the carbon matrix.

At higher temperature (≈800°C), ZnO is reduced by the carbon phase and the formed Zn(0) leaves again the sample as vapour phase. As a result, a holed carbon phase is generated, whose surface has been imprinted by ZnO microcrystals previously present.

## Acknowledgments

The authors thank MIUR and INSTM Consorzio for their economical support. The authors would like to thank also Dr. Marco Zanetti for the FTIR analysis.

## References

- Bertarione S., Bonino, F., Damin, A. 2007. Polymerization of Furfuryl Alcohol in the space-limited H-Y zeolite: FTIR, Raman and UV-visible studies.in preparation.
- Birks L.S., Friedman, H. 1946. Particle size Determination from X-Ray Line Broadening. *Journal of Applied Physics*. 17(8):687-692.
- Calleja J.M., Cardona, M. 1977. Resonant Raman scattering in ZnO. *Physical Review B*. 16(8):3753-3761.
- Cesano F., Domenica, S., Bertarione, S., et al. 2007. ZnO-Carbon composites and imprinted carbon by pyrolysis of ZnCl<sub>2</sub>-catalyzed furfuryl alcohol polymers. *Submitted to Carbon*.
- Choura M., Belgacem, N.M., Gandini, A. 1996. Acid-catalyzed polycondensation of furfuryl alcohol: Mechanisms of chromophore formation and cross-linking. *Macromolecules*. 29(11):3839-3850.
- Conley R.T., Metil, I. 1963. An investigation of the structure of furfuryl alcohol polycondensates with infrared spectroscopy. *Journal of Applied Polymer Science*. 7(1):37-52.
- Dunlop A.P., Peters, F.N. 1953. The Furans. New York: Reinhold Publishing Co.
- Foley H.C. 1995. Carbogenic Molecular-Sieves - Synthesis, Properties and Applications. *Microporous and Mesoporous Materials*. 4(6):407-433.
- Gonzalez R., Figueroa, J.M., Gonzalez, H. 2002. Furfuryl alcohol polymerisation by iodine in methylene chloride. *European Polymer Journal*. 38(2):287-297.
- Johnson D.J., Tison, C.N. 1969. The fine structure of graphitized fibres. *Brit J Appl Phys (J Phys D)*. 2(2):787-897.
- Petkov V., DiFrancesco, R.G., Billinge, S.J.L., et al. 1999. Local structure of nanoporous carbons. *Philosophical Magazine B-Physics of Condensed Matter Statistical Mechanics Electronic Optical and Magnetic Properties*. 79(10):1519-1530.
- Pierson H.O. In: Pierson HO, ed. *Handbook of Carbon, Graphite, Diamond and Fullerenes - Properties, Processing and Applications*. Park Ridge, New Jersey, U.S.A: William Andrew Publishing/Noyes 1993:399.
- Principe M., Ortiz, P., Martinez, R. 1999. An NMR study of poly(furfuryl alcohol) prepared with p-toluenesulphonic acid. *Polymer International*. 48(8):637-641.
- Robertson J. 2002. Diamond-like amorphous carbon. *Materials Science & Engineering R-Reports*. 37(4-6):129-281.
- Rodriguez-Mirasol J., Cordero, T., Radovic, L.R., et al. 1998. Structural and textural properties of pyrolytic carbon formed within a microporous zeolite template. *Chemistry of Materials*. 10(2):550-558.
- Sthel M., Rieumont, J., Martinez, R. 1999. Testing a furfuryl alcohol resin as a negative photoresist. *Polymer Testing*. 18(1):47-50.
- Strano M.S., Zydney, A.L., Barth, H., et al. 2002. Ultrafiltration membrane synthesis by nanoscale templating of porous carbon. *Journal of Membrane Science*. 198(2):173-186.
- Sugama T., Kukacka, L.E., Carciello, N., et al. 1985. Adhesion aspects of levulinic-acid-modified furan polymers to crystalline zinc phosphate metal surface. *Journal of Applied Polymer Science*. 30:2137-2155.
- Vergunst T., Kapteijn, F., Moulijn, J.A. 2002. Preparation of carbon-coated monolithic supports. *Carbon*. 40(11):1891-1902.
- Wang Z., Lu, Z., Huang, X., et al. 1998. Chemical and crystalline structure characterizations of polyfurfuryl alcohol pyrolyzed at 600 degrees C. *Carbon*. 36(1-2):51-59.

- Zarbin A.J.G., Bertholdo, R., Oliveira, M. 2002. Preparation, characterization and pyrolysis of poly(furfuryl alcohol)/porous silica glass nanocomposites: novel route to carbon template. *Carbon*. 40(13):2413-2422.
- Zerbi G., Tommasini, M., Centrone, A., et al. A spectroscopic approach to carbon materials for energy storage. *Carbon: The Future Material for Advanced Technology Applications*. Berlin: SPRINGER-VERLAG BERLIN 2006:23-53.